Classification of ECG signal during Atrial Fibrillation using Naive Bayes model

María de la Paz Cardona CID:01410045

I. Introduction

Cardiovascular diseases (CVDs) are a leading cause of death that threaten especially the health of middle-aged and old people [1]. The aging population the world is facing makes it imperative to find better ways to diagnose and treat these diseases. Amongst CDVs we find cardiac arrhythmia, which is characterised by the heart beating too fast, too slowly, or with an irregular rhythm. Amongst the 12 leading types of arrhythmia [2], atrial fibrillation (AF) is the most encountered in clinical practice [3]. AF occurs when the atria beat chaotically and irregularly, out of sync with the ventricles [4]. Moreover, it prevents blood from being ejected completely out of the atria, which can cause blood clots and increase the risk of stroke. [5].

An electrocardiograph (ECG) is a test that can be used to detect and diagnose cardiac arrhythmia by measuring heart rhythm and electrical activity. This non-invasive method is easy to operate and is used routinely in clinical applications. However, the judgement of cardiovascular diseases by visually assessing an ECG is not always perfectly accurate and heavily depends on the doctor's experience. By computerising electrocardiogram classification, human errors and healthcare costs can be reduced, helping with early prevention, timely detection and proper treatment [5].

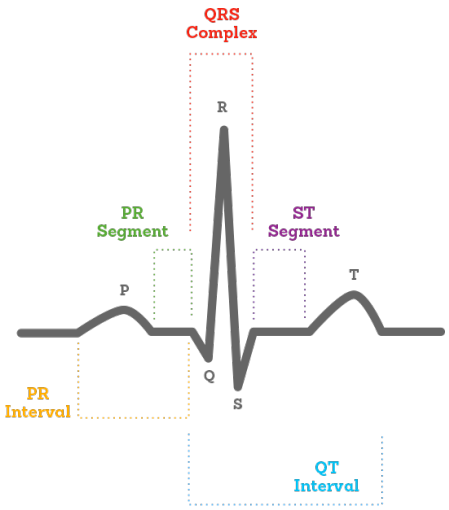

Figure 1. Schematic of an ECG cycle, showing the different waves and peaks [6].

ECG can be a particularly useful tool for AF detection since it shows distinct morphological features when patients suffer from it. To understand these features it is important to first define the characteristics of a typical ECG signal. For a healthy individual, this signal is approximately periodic (a sign of a regular rhythm), and in each of the periods, the waves and peaks identified in Figure 1 can be observed.

Starting from the right, we can observe the P wave, representing wave depolarisation spreading from the SA node throughout the atria. In AF, this wave cannot be seen or may be observed as "coarse fibrillatory waves" on the ECG, i.e. oscillations in amplitude around the baseline dependent on the magnitude of the underlying voltage [7]. The P wave is followed by the QRS complex, the period between them is termed the PR interval and represents the time between the onset of atrial depolarisation and the onset of ventricular depolarisation. The QRS complex represents ventricular depolarisation. Ventricular rate can be calculated from the time interval between QRS complexes; in AF patients this rate is variable. Additionally, patients with AF show a wide QRS complex ($\geq$ 120 ms). This condition represents a slower spread of ventricular depolarisation [8]. The isoelectric period (ST segment), which follows the QRS and ends just before the beginning of the T wave, is the time at which both ventricles are completely depolarized. Finally, the T wave represents ventricular re-polarisation and, generally, exhibits a positive deflection [9]. Figure 2 shows a comparison of the ECGs of a healthy and an AF patient.

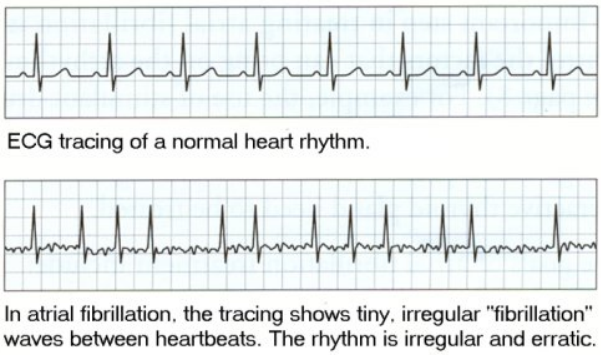

Figure 2. Side by side comparison of an ECG signal from a healthy individual (top) against one who suffers from AF (bottom). Observe the regular periodic signal on the top versus the irregular fibrillatory signal on the bottom [10].

The morphological features mentioned above have enabled the development of traditional cardiac rhythms classification methods based on signal processing and frequency domain analysis. There exist some real-time modern filtering methods, such as the Wiener filter, that make use of the time domain analysis [11]. Novel approaches of cardiac classification from ECG signals make use of machine learning algorithms such as neural networks [12]. This report compares the performance of two probabilistic reasoning classifiers, a Naïve Bayes Model and a Gaussian Mixture Model.

II. Methods

Below is a flowchart summarising the processes carried out for the analysis and classification of the data.

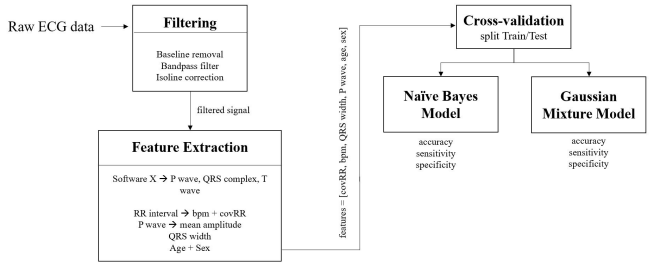

Figure 3. Diagram summarising data analysis method.

A. Filtering

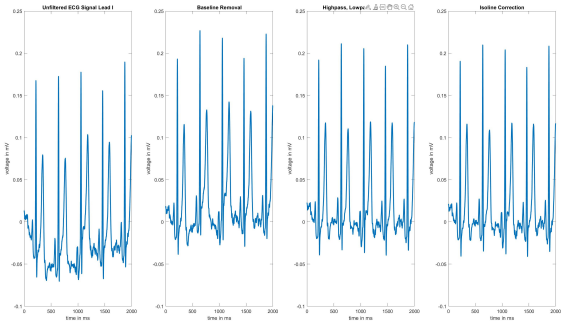

Figure 4. ECG signal of patient 'A0030' after each of the filtering steps.

The first step was filtering the raw ECG data to remove noise and artefacts. The filtering functions used are from the Open Access Software publication Software X [13]. First, a baseline removal filter, `ECG_Baseline_Removal()`, was applied to the signal to remove baseline wander. This is an artefact that corrupts the ECG, hindering the correct diagnosis of cardiac diseases [14]. After removing the baseline wander, the signal was filtered with `ECG_High_Low_Filter()` and `Notch_Filter()`. These perform bandpass filtering, which can help reduce the baseline drift, motion artifacts and high frequency noise. Correct selection of the filter frequencies can ease isolation of the high-frequency QRS complex against the low-frequency P and T waves and remove low-frequency noise and 50 Hz powerline artefacts [15]. The frequencies selected were 120 Hz for the lowpass, 0.3 Hz for the highpass, and bandstop 49-51 Hz. Finally, isoline drift correction was applied using `Isoline_Correction()`. All functions are grouped together in `filtering_ecg()`, which is called in the pre-processing function `pre_processing2()`.

B. Feature Extraction

The next step was to extract the features from the ECG signals. P waves, QRS complexes and T waves were extracted using open-source code from Software X [13], the result is shown in Figures 5 and 6. From these waves, specific features were extracted, which were then used as an input to the classifiers to help identify AF patients.

To detect the lack of P waves present in AF, the mean amplitude at the highest point of each P wave was calculated. For AF patients this value is expected to be close to 0, i.e. no P waves detected, but not for healthy patients. Additionally, the QRS complexes were used to extract the RR interval (the distance between R peaks), which was used to calculate the heart rate. This is normally about 50-100 but can go up to 100 bpm in AF [16]. The covariance of RR interval was also calculated to get a sense of rhythm regularity, expecting high covariance for irregular AF rhythms and low covariance for regular healthy rhythms. Finally, from the QRS complex, the width (distance from Q to S) was calculated. As mentioned before, QRS complexes are wider in AF ($\geq$ 120 ms).

Furthermore, age and sex from the .mat files were added as extra features for the classification. There exists a strong correlation between AF and age of the patients who suffer from it since approximately 70% of them are between 65 and 85 years of age [17]. As for gender, the incidence of AF is greater in men than in women, but this gap closes with advancing age [18]. The feature extraction function, `Annotate_ECG_Multi()`, is called in `pre_processing2()`.

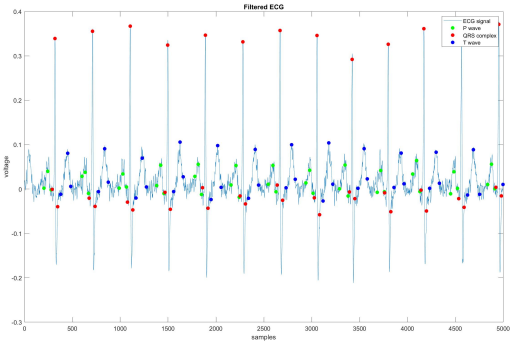

Figure 5. P waves, QRS complex and T waves for ECG of healthy patient 'A0002'.

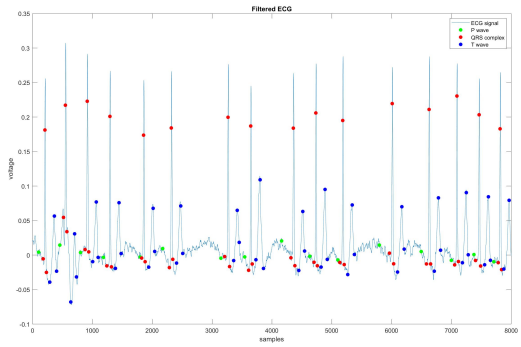

Figure 6. P waves, QRS complex and T waves for ECG of AF patient 'A0009'. Observe how there are few P waves identified and these have a very low, close to 0, amplitude. Also note the irregular RR intervals.

C. Classification

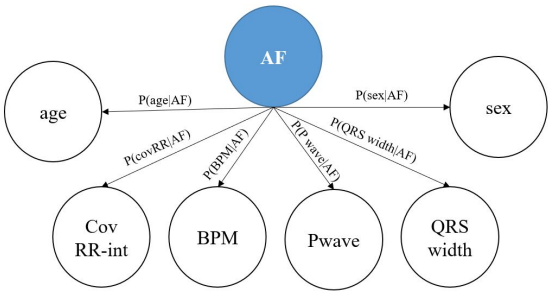

Figure 7. Directed Graph for Naive Bayes Classifier.

1) Naïve Bayes Classifier: ECG classification was first performed through a Naïve Bayes model using `fitcnb()`. This model was chosen because, despite its simplicity, it has provided successful results in similar ECG classifications [19]–[21]. The Naïve Bayes model uses Bayes' theorem to predict the most likely class from a data sample's features [22]. Bayes' theorem defines the posterior probability $P(AF|X)$ as:

$$P(AF|X) = \frac{P(AF)P(X|AF)}{P(X)} \tag{1}$$

where X represents the vector of features [covRR, bpm, QRS width, P wave, age, sex]. Since features are assumed to be independent, the likelihood can be expressed as:

$$P(X|AF) = \prod_{i=1}^{6} P(x_i|AF) \tag{2}$$

Equation (2) can be substituted in Equation (1) giving:

$$P(AF|X) = \alpha P(AF) \prod_{i=1}^{6} P(x_i|AF) \tag{3}$$

where α is the normalisation constant.

Figure 7 shows the directed graph for this model. In this two-class classification problem, the aim is to determine whether a patient has AF (class 1) or not (class 0) given the set of features extracted in the previous step. The link matrices below can help calculate the likelihoods needed to determine the posterior, as shown in the previous equations.

$$P(age|AF) =$$

$$\begin{bmatrix} P(age = young|AF = no) & P(age = old|AF = no) \\ P(age = young|AF = yes) & P(age = old|AF = yes) \end{bmatrix}$$

$$P(covRR|AF) =$$

$$\begin{bmatrix} P(covRR = low|AF = no) & P(covRR = high|AF = no) \\ P(covRR = low|AF = yes) & P(covRR = high|AF = yes) \end{bmatrix}$$

$$P(bpm|AF) =$$

$$\begin{bmatrix} P(bpm = low|AF = no) & P(bpm = high|AF = no) \\ P(bpm = low|AF = yes) & P(bpm = high|AF = yes) \end{bmatrix}$$

$$P(Pwave|AF) =$$

$$\begin{bmatrix} P(Pwave = no|AF = no) & P(Pwave = yes|AF = no) \\ P(Pwave = no|AF = yes) & P(Pwave = yes|AF = yes) \end{bmatrix}$$

$$P(QRS\_width|AF) =$$

$$\begin{bmatrix} P(QRS\_width = small|AF = no) & P(QRS\_width = large|AF = no) \\ P(QRS\_width = small|AF = yes) & P(QRS\_width = large|AF = yes) \end{bmatrix}$$

$$P(sex|AF) =$$

$$\begin{bmatrix} P(sex = female|AF = no) & P(sex = male|AF = no) \\ P(sex = female|AF = yes) & P(sex = male|AF = yes) \end{bmatrix}$$

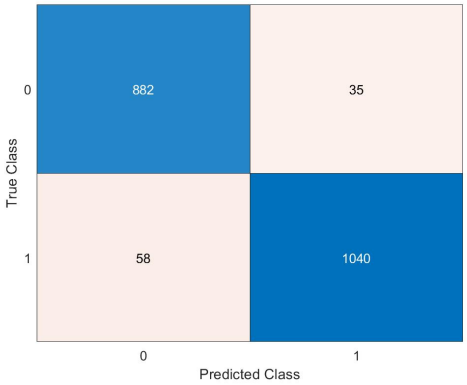

Figure 8. Confusion matrix. 0 represents healthy and 1 represents AF.

Initially, classification was performed considering only lead II. From the confusion matrix above, the following values were obtained: accuracy = 0.9538, sensitivity = 0.9618, and specificity = 0.9472.

Classification was then repeated using the 12 different leads and their accuracy, sensitivity, and specificity values were compared to determine which leads yield better classification results. Results are summarised in the table below.

Lead	Accuracy	Sensitivity	Specificity
I	0.9538	0.9433	0.9627
II	0.9538	0.9618	0.9472
III	0.9250	0.9443	0.9089
aVR	0.9543	0.9433	0.9636
aVL	0.8948	0.9040	0.8871
aVF	0.9290	0.9542	0.9080
V1	0.8998	0.9140	0.8871
V2	0.9225	0.9596	0.8914
V3	0.8857	0.8975	0.8759
V4	0.9453	0.9629	0.9489
V5	0.8838	0.8877	0.8805
V6	0.8761	0.9727	0.7951

Table I
EVALUATION METRICS FOR DIFFERENT ECG LEADS.

Lead II, which gave the best accuracy and sensitivity, was determined to be the optimal lead for this classifier. In clinical practice, it is the most used to record the rhythm strip since it usually gives a good view of the P wave [23]. Classification accuracy on this lead was further explored by performing 10-fold cross-validation. Mean accuracy was found to be 0.9553 and standard deviation to be 0.0212. To further improve the accuracy, the classification on lead II was optimised by finding the best hyperparameters. Instead of normal (Gaussian) distribution, distribution was changed to a Kernel smoothing density estimate with width 10.502. After specifying this, mean accuracy when up to 0.9826 and standard deviation decreased to 0.0067.

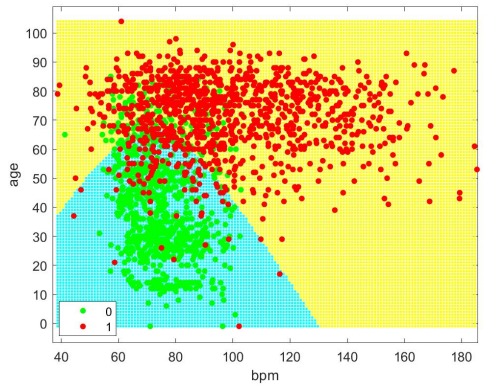

Figure 9. Decision surface of Naïve Bayes classifier using two features.

2) Gaussian Mixture Model: A Gaussian Mixture Model (GMM) was also implemented, `fitgmdist()`. This model was chosen because it is a probabilistic reasoning classifier that has provided successful results in similar ECG classifications [24], [25]. GMM implements the Expectation-Maximisation (EM) algorithm for fitting a mixture of, in this case, two Gaussian models:

$$p(x|\alpha_1, \alpha_2, \mu_1, \mu_2, \sigma_1, \sigma_2) = \alpha_1 \frac{1}{\sigma_1\sqrt{2\pi}} e^{-\frac{(x-\mu_1)^2}{2{\sigma_1}^2}} + \alpha_2 \frac{1}{\sigma_2\sqrt{2\pi}} e^{-\frac{(x-\mu_2)^2}{2{\sigma_2}^2}} \quad (4)$$

EM first calculates the expectation of the component assignments C_k for each data point $x_i \in X$, given the model parameters α_k, μ_k, and σ_k. It then maximises the expectations with respect to the model parameter, iteratively updating the values α_k, μ_k, and σ_k. When the algorithm converges, it gives a maximum likelihood estimate. One advantage of GMM is that it is a form of unsupervised learning, meaning it could be trained with unclassified data. The number of distributions, i.e. 2, was set using Akaike's Information Criterion (AIC) by selecting the number of components that gave a lower AIC. When performing 10-fold cross-validation on lead II, a mean accuracy of 0.4802 and a standard deviation of 0.4789 were obtained. The values obtained for sensitivity and specificity were 0.4248 and 0.4244 respectively. These results are worse than those obtained with the Naïve Bayes model, as shown in Figure 11.

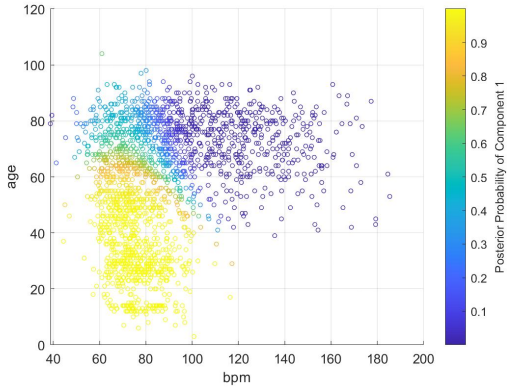

Figure 10. Decision surface for GMM using two features. The plot displays the posterior probability of having AF, i.e. 1 for having AF, 0 for not having it. Note the number of data points for which the posterior probability is at an intermediate value, showing how the classifier is unsure about these points. This is reflected by the lower accuracy obtained.

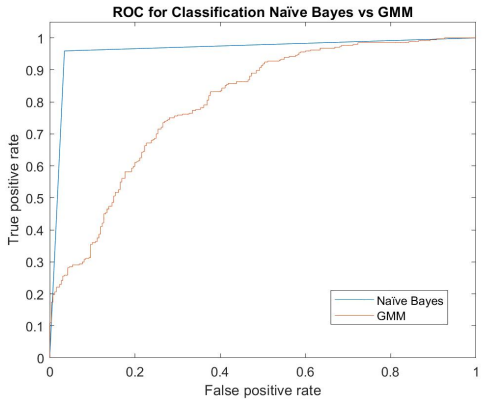

Figure 11. ROC curve for both classifiers implemented. This graph clearly shows the superior performance of the Naïve Bayes classifier against the GMM.

III. Discussion

Naïve Bayes model proved to be a satisfactory classifier for determining whether a patient has AF from their ECG features, obtaining high accuracy, sensitivity, and specificity values. By performing cross-validation it was ensured that these high percentages were not a result of over-fitting and that the classifier would successfully classify new unseen data. The low standard deviation, 0.0067, is a sign that the classifier consistently achieves accuracies close to the mean value of 0.9826. A characteristic of Naïve Bayes classifier is that it assumes that the features selected are conditionally independent, which might not be necessarily true in this scenario. As a future development, a bayesian classifier that does not make this assumption could be implemented.

Some difficulties and challenges were encountered during the feature extraction and classification processes. Currently, the open-source code for feature extraction takes a relatively long processing time of up to 3 minutes. This could be improved by some further optimisation. Moreover, not all the features can be extracted for every patient and every lead, meaning that the table containing the features needed to be cleaned before the classification.

`main_multiple_leads()` contains a variation of the main script (filtering, feature extraction and classification), where features are extracted from the leads that gave better results in Table 1 (I, II, aVR and V4) and the average feature values are calculated across them. Before the optimisation of the Naïve Bayes classifier, this combination gives better results (accuracy: 0.9702, sensitivity: 0.9638 and specificity: 0.9717, versus before 0.9538, 0.9618, 0.9472). But not after optimisation (mean accuracy: 0.9747 and standard deviation 0.0064, versus before 0.9826 and 0.0067). Future development would involve analysing the different leads and extracting features according to which lead captures each feature the best and taking an average across leads that successfully extract the same features.

For the GMM classification, the results obtained were relatively unreliable since every time the algorithm was run it gave different results, as reflected in the high standard deviation (0.4789). When performing cross-validation, mean accuracy varied from 0.2 to 0.6, though most of the times results were around 0.4-0.5. This accuracy is not suitable for clinical practice and the model should be further modified since GMM has proved to achieve satisfactory results, even surpassing the Naïve Bayes classifier [24]. Moreover, the model would sometimes crash because of ill-conditioned covariance caused by a strong correlation between the features. This could be fixed by applying independent component analysis (ICA) to the data before classification. These issues did not improve when combining leads, though overall accuracy went up to 0.6910, standard deviation was 0.4641, showing the variation in the accuracies obtained. Eventually, the result of both classifiers could be combined through techniques such as Bagging [26] and Boosting [27].

IV. Conclusion

The results obtained show successful classification of patients with atrial fibrillation, using a Naïve Bayes classifier. Although an overall accuracy of 0.9826 was obtained, there is still room for improvement by optimising the feature extraction and upgrading the GMM. MATLAB code is available on: https://github.com/mdc5017/SPN_sensing_exercise.

References

[1] Kevin McNamara, Hamzah Alzubaidi, and John Jackson. Cardiovascular disease as a leading cause of death: how are pharmacists getting involved? *Integrated Pharmacy Research and Practice*, Volume 8:1–11, 02 2019.

[2] Henrik Haraldsson, Lars Edenbrandt, and Mattias Ohlsson. Detecting acute myocardial infarction in the 12-lead ecg using hermite expansions and neural networks. *Artificial Intelligence in Medicine*, 32(2):127–136, 2004.

[3] Leif Sörnmo, Martin Stridh, Daniela Husser, Andreas Bollmann, and S. Olsson. Analysis of atrial fibrillation: From electrocardiogram signal processing to clinical management. *Philosophical transactions. Series A, Mathematical, physical, and engineering sciences*, 367:235–53, 11 2008.

[4] Atrial fibrillation, mayo foundation for medical education and research. =https://www.mayoclinic.org/diseases-conditions/atrial-fibrillation, Oct 2021.

[5] K. Padmavathi and K. Sri Ramakrishna. Classification of ecg signal during atrial fibrillation using autoregressive modeling. *Procedia Computer Science*, 46:53–59, 2015. Proceedings of the International Conference on Information and Communication Technologies, ICICT 2014, 3-5 December 2014 at Bolgatty Palace Island Resort, Kochi, India.

[6] What is an ecg?. alivecor uk. https://www.alivecor.com/education/ecg.html. Accessed: 2021-11-30.

[7] Zhao TX;Martin CA;Cooper JP;Gajendragadkar PR;. Coarse fibrillatory waves in atrial fibrillation predict success of electrical cardioversion.

[8] Behzad Pavri. Differential diagnosis of wide qrs complex tachycardias. =https://www.thecardiologyadvisor.com/home/decision-support-in-medicine/cardiology/differential-diagnosis-of-wide-qrs-complex-tachycardias/, journal=The Cardiology Advisor, Jan 2019.

[9] Richard E. Klabunde. *Cardiovascular Physiology Concepts*. Wolters Kluwer, 2022.

[10] Diagnosis and treatment of atrial fibrillation, chest heart and stroke scotland. https://www.chss.org.uk/heart-information-and-support/about-your-heart-condition/common-heart-conditions/heart-arrhythmias-2/medical-treatment-atrial-fibrillation/. Accessed: 2021-11-28.

[11] Manju Bala and Sneha M.R. Ecg denoising using wiener filter and kalman filter. *Procedia Computer Science*, 171:273–281, 01 2020.

[12] Jiacheng Wang and Weiheng Li. Atrial fibrillation detection and ecg classification based on cnn-bilstm. 11 2020.

[13] Softwarex. https://www.journals.elsevier.com/softwarex. Accessed: 2021-11-30.

[14] Gustavo Lenis, Nicolas Pilia, Axel Loewe, Walther H W Schulze, and Olaf Dössel. Comparison of baseline wander removal techniques considering the preservation of st changes in the ischemic ecg: A simulation study. *Computational and Mathematical Methods in Medicine*, 2017:1–13, 03 2017.

[15] Aleksandr Fedotov. Selection of parameters of bandpass filtering of the ecg signal for heart rhythm monitoring systems. *Biomedical Engineering*, 50, 09 2016.

[16] Atrial fibrillation, nhs choices. https://www.nhs.uk/conditions/atrial-fibrillation/. Accessed: 2021-11-30.

[17] William M. Feinberg, Joseph L. Blackshear, Andreas Laupacis, Richard Kronmal, and Robert G. Hart. Prevalence, Age Distribution, and Gender of Patients With Atrial Fibrillation: Analysis and Implications. *Archives of Internal Medicine*, 155(5):469–473, 03 1995.

[18] Ezekowitz M. D. Michelena, H. I. Atrial fibrillation: are there gender differences? *The journal of gender-specific medicine : JGSM : the official journal of the Partnership for Women's Health at Columbia*, 3(6):44–49, 2000.

[19] s Padmavathi and Ramanujam Elangovan. Naïve bayes classifier for ecg abnormalities using multivariate maximal time series motif. *Procedia Computer Science*, 47:222–228, 12 2015.

[20] S. Aarthy and J. Iqbal. Time series real time naive bayes electrocardiogram signal classification for efficient disease prediction using fuzzy rules. *Journal of Ambient Intelligence and Humanized Computing*, 12, 05 2021.

[21] S. Celin and K. Vasanth. Detection and classification of r-peak using naïve bayes classifier. *International Journal of Engineering and Technology(UAE)*, 7:397–403, 08 2018.

[22] Irina Rish et al. An empirical study of the naive bayes classifier. In *IJCAI 2001 workshop on empirical methods in artificial intelligence*, volume 3, pages 41–46, 2001.

[23] Steve Meek and Francis Morris. Abc of clinical electrocardiography: Introduction. i—leads, rate, rhythm, and cardiac axis. *BMJ (Clinical research ed.)*, 324:415–8, 03 2002.

[24] Roshan Martis, U Rajendra Acharya, Hari Prasad, Kuang Chua, and Choo Lim. Automated detection of atrial fibrillation using bayesian paradigm. *Knowledge-Based Systems*, 54:269–275, 12 2013.

[25] Mehmet İşcan, Cüneyt Yilmaz, and Faruk Yiğit. Arrhytmic and non-arrhytmic heartbeat classification based on gaussian mixture model. In *2016 Electric Electronics, Computer Science, Biomedical Engineerings' Meeting (EBBT)*, pages 1–4, 2016.

[26] Leo Breiman. Bagging predictors. machine learning. 26:123–140, 1994.

[27] Yoav Freund and Robert E. Schapire. Experiments with a new boosting algorithm. *ICML*, 1996.